Mechanistic Study of the Electrochemical Oxygen Reduction Reaction on Pt(111) Using Density Functional Theory

Matthew P. Hyman and J. Will Medlin*

Department of Chemical and Biological Engineering, University of Colorado, Boulder, Colorado 80309

Received: March 23, 2006; In Final Form: May 18, 2006

Density functional theory (DFT) was used to study the electrolyte solution effects on the oxygen reduction reaction (ORR) on Pt(111). To model the acid electrolyte, an $H_5O_2^+$ cluster was used. The vibrational proton oscillation modes for adsorbed $H_5O_2^+$ computed at 1711 and 1010 cm^{-1}, in addition to OH stretching and H_2O scissoring modes, agree with experimental vibrational spectra for proton formation on Pt surfaces in ultrahigh vacuum. Using the $H_5O_2^+$ model, protonation of adsorbed species was found to be facile and consistent with the activation barrier of proton transfer in solution. After protonation, OOH dissociates with an activation barrier of 0.22 eV, similar to the barrier for O_2 dissociation. Comparison of the two pathways suggests that O_2 protonation precedes dissociation in the oxygen reduction reaction. Additionally, an OH diffusion step following O protonation inhibits the reaction, which may lead to accumulation of oxygen on the electrode surface.

1. Introduction

The poor oxygen reduction kinetics on Pt electrodes has motivated the study of oxygen reduction on Pt alloys.[1−4] However, the lack of a mechanistic understanding of the oxygen reduction reaction (ORR) has hindered progress in catalyst design. This elusiveness is largely a result of the inaccessibility of the electrode|electrolyte interface to surface probes. Thus, researchers have relied on electrochemical techniques to indirectly probe the surface chemistry. The conflicting data and corresponding proposed mechanisms have been reviewed previously.[5,6] To briefly summarize here, Damjanovic et al. originally proposed that proton transfer occurs simultaneously with charge transfer after the initial adsorption of molecular oxygen.[7,8] This was based on early rotating disk electrode studies which indicated that the initial electron transfer is rate limiting and revealed Temkin kinetics at low current densities, but Langmuir kinetics at high current densities. Based on their derivation of the coverage-dependent activation energy, the authors reasoned that the transition from Temkin to Langmuir kinetics, together with the transition from a fractional order dependence of pH to a dependence of unity, demonstrates that the simultaneous charge transfer and proton transfer is rate limiting. The Temkin kinetic regime was explained by OH_{ad} accumulation on the surface.[9] More recently, it has been proposed that high OH_{ad} coverages originate predominantly from water dissociation at potentials >0.8 V vs RHE (reversible hydrogen electrode) on Pt electrode rather than from the ORR itself.[10] It has also been proposed that the reaction proceeds through a peroxide intermediate based on rotating ring disk electrode studies that detect peroxide formation,[11] which supports the argument that protonation precedes dissociation. An alternate view, proposed by Yeager et al. and based on kinetic isotope experiments, is that oxygen adsorbs dissociatively, but corroborating evidence is lacking.[5,12] Additionally, Yeager speculated that O_2 adsorption could possibly be the rate-determining step.[5]

Much work has been previously performed to study behavior of oxygen on Pt(111)[13−21] and its reaction with hydrogen in a vacuum.[22−31] However, the presence of the electrolyte solution and the resulting electric double layer (EDL) at electrode|solution interfaces complicate the extraction of pertinent information from these studies. The EDL is the result of charge accumulation on the metal electrode surface and counter charge in the solution upon the application of an electrode potential.[32,33] One approach to bridging the gap between the metal|vacuum interface and the electrode|solution interface is to simulate the EDL in ultrahigh vacuum. While arguments have been made in favor of this technique,[34] it is unclear whether any results relevant to the oxygen reduction reaction can be obtained through vacuum simulations. In ultrahigh vacuum (UHV), water molecules adsorb in a hexagonal structure due to hydrogen bonding,[35,36] and desorb at ca. 180 K.[22,24,30] It is well-known that hydrogen bonding decreases as temperature increases,[37,38] so the validity of this hexagonal model at temperatures above 300 K should be questioned. Additionally, oxygen adsorption on Pt(111) at low temperatures is severely hindered by adsorbed water and does not occur at all at H_2O coverage > 0.8 monolayer (ML).[39]

Ultrahigh vacuum studies may, however, help reveal the nature of the proton at the metal|solution interface. (The term "proton" is used loosely to refer to $H^+(H_2O)_n$, where $n = 0, 1, 2, ...$) The coadsorption of hydrogen and water on Pt(111),[40] Pt(110),[41] and Pt(100)[42] single crystals has been studied by several groups using electron energy loss spectroscopy (EELS). On all three of these surfaces, two vibrational modes were assigned to the formation of the proton: a mode near 1150 cm^{-1} and a mode in the range of 1680−1730 cm^{-1}. Initially, the proton structure was identified as H_3O^+,[40] although the structure is likely a dihydrated proton ($H_5O_2^+$) or a trihydrated hydronium ion ($H_9O_4^+$).[41] Wagner and Moylan estimated that up to 1/8 ML of H_{ad} can form "H_3O^+" when reacted with H_2O,[40] while Kizhakevariam et al. estimated more conservatively that the "H_3O^+" surface coverage is >0.05 ML.[42] In situ infrared reflection absorption spectroscopy (IRAS) has also been performed to study proton interaction with Pt surfaces. Hirota et

* Corresponding author. E-mail: will.medlin@colorado.edu.

10.1021/jp061813y CCC: $33.50
Published on Web 07/14/2006

al., performing experiments on Pt(111) in 0.1 M $HClO_4$, 0.1 M HF, and 0.5 M H_2SO_4, used the study by Wagner and Moylan to assign a vibrational mode as belonging to "H_3O^+".[43] However, performing similar experiments on Pt(111) in 0.1 $HClO_4$, Iwasita and Xia did not assign any modes to a surface proton structure. Unfortunately, ab initio studies of "H_3O^+" on metal surfaces are lacking. Olivera et al. studied hydrated hydronium ions on Ag(111) using MP2 cluster models.[44] The results indicate that H_3O^+ is stable on Ag(111), but that hydration of the bare hydronium is energetically favorable.

The vibrational studies suggest the existence of protonated water molecules, but they are not able to identify the surface structure. Further insight can be gained by considering the behavior of protons in liquid water, as opposed to water molecules at an electrode surface. The proton diffusion mechanism in liquid water was first proposed by Grotthus in 1806.[45] Since then, two proton structures have been proposed: a proton shared by two H_2O molecules, known as the Zundel structure ($H_5O_2^+$),[46] and a hydronium ion strongly hydrogen bonded to three H_2O molecules, known as the Eigen structure ($H_9O_4^+$).[47] Ab initio molecular dynamics simulations indicate that these two structures are only limiting structures, and that numerous other proton structures exist between these two limits.[48] Regardless, protons can be transferred from Zundel to Zundel, Eigen to Eigen, Eigen to Zundel, and Zundel to Eigen structures.[48,49] Proton transfer between Zundel structures involves oscillation of the proton between water molecules and is approximately activationless. Proton transfer from an Eigen structure involves breaking a hydrogen bond in the second hydration shell, which then allows the transfer of a proton from the hydronium core. The proton diffusion process is rate limited by the hydrogen bond breaking step, which has an activation energy of ca. 0.11 eV.[49,50] A recent combined experimental/theoretical study has provided further insight into the structures of these proton complexes.[51] This study found the proton oscillation between two water molecules in a Zundel cluster is responsible for an absorption band at 1085 cm^{-1}, with a mode resulting from the bending of the two water molecules at 1770 cm^{-1}. The absorption modes of the Eigen structures vary significantly depending on the number of solvating molecules, with the $H_9O_4^+$ configuration characterized by very strong absorption at 2665 cm^{-1}. However, the 1085 cm^{-1} mode is unique to the Zundel structure.

As mentioned above, both experimental and theoretical studies have exhaustively explored the behavior of oxygen and its reaction with hydrogen on Pt surfaces. Previously, we examined the effect of homogeneous electric fields on oxygen adsorption and dissociation on Pt(111) with density functional theory (DFT)[52,53] to model the electrostatic effect of the EDL.[54] With a Pt(111) slab model, which exhibits good experimental agreement of the dipole moments, we found that the electric field has a negligible effect on the dissociation reaction energy. However, imposing an electric field does alter the dissociation barrier. An electric field of the magnitude found at fuel cell cathodes (0.5 V/Å) increases the dissociation barrier by ca. 0.1 eV. While no categorical conclusions can be drawn from this, it indicates that the molecular oxygen dissociation rate should decrease with increasing potential.

In the current study, we examine oxygen reduction on Pt(111) using density functional theory, focusing on the effect of the electrolyte solution on elementary surface reaction steps. In these investigations, a simple Zundel structure has been used to model the solvated protons that participate in the various elementary reaction steps. As discussed below, the Zundel model appears to be the simplest solution model consistent with the available experimental data. Rather than trying to recreate the entire electrode|electrolyte interface, we attempt to recreate key features of the UHV model of the interface using DFT. This allows for the study of the fundamental electrochemical proton transfer and dissociation steps in a UHV-like manner. This paper does not comprehensively examine the full surface effects (i.e., adsorbate repulsion), nor does it consider the solvent reorganization steps necessary for the complete catalytic sequence. Rather, it focuses on the fundamental steps to begin to understand the role of the solution at the interface, evaluate the reaction mechanisms proposed by Damjanovic and Yeager, and identify any steps that may contribute to the slow reaction kinetics. Additionally, information from this study enables a more thorough study of the electrostatic effects of the EDL, which will be published in the future. Ideally, with this information, a more detailed and accurate picture of the ORR can be constructed.

2. Methods

In choosing a model for the solution, several possibilities were considered. The simplest of these, the bare hydronium ion, was found not to be stable on Pt(111). Instead of adsorbing, the H_3O^+ molecule decomposes to H_{ad} hydrogen bonded to H_2O, which does not interact directly with the Pt surface. The $H_{ad}-O$ distance in this configuration is 1.90 Å. This result suggests that the solvating effects of a single H_2O molecule are insufficient to stabilize H as a proton; instead, it is adsorbed on the surface as atomic H. We note that H_3O^+ was determined to be stable on Ag(111),[44] but that this discrepancy can perhaps be explained by the low affinity of silver for atomic hydrogen.[55,56]

Also considered as solution models were variations of the Zundel and Eigen clusters. Preliminary investigations indicated that proton transfer to molecular oxygen could only be readily achieved from the basic Zundel cluster consisting of a proton solvated by two water molecules. The lack of proton transfer from the other structures is likely due to the strong hydrogen bonding between the core structures ($H_5O_2^+$, H_3O^+) and the solvating water molecules that are anchored to the Pt surface, stabilizing the ions.[57] Considering the inaccessibility of the proton/hydronium ion in the large hydrated clusters, we speculate that proton transfer may preferentially occur through the simple Zundel cluster. The Zundel structure is also consistent with observed vibrational spectra, as discussed below. On the basis of our calculations and the spectroscopic data discussed previously, we selected the simple Zundel ($H_5O_2^+$) cluster to model proton transfer in the EDL.

The calculations in this study were performed using the Vienna Ab initio Software Program (VASP),[58−60] which uses density functional theory to calculate electronic energies for periodic systems. Plane waves of energies up to 400 eV were constructed using the projector augmented wave (PAW) method.[61,62] The generalized gradient approximation (GGA) was implemented using the PW91 functional.[63] A $5 \times 5 \times 1$ Monkhorst−Pack *k*-point mesh was used to sample the Brillouin zone.[64] Electron occupancies were determined using Gaussian smearing with a width of 0.2 eV, while the total energies were extrapolated to 0 eV. The $O_2/H_5O_2^+$ and $OOH/(H_2O)_2$ calculations were performed both with and without spin polarization since top−bridge−top adsorbed O_2 on clean Pt(111) is paramagnetic.[13]

In most of the calculations, a 3×3 Pt(111) unit cell was used. The unit cell consisted of three frozen Pt layers with a

calculated lattice constant of 3.99 Å and 16.1 Å of vacuum space. One $H_5O_2^+$ cluster was adsorbed per unit cell for the electrochemical calculations. Geometry optimization calculations were performed with a force criterion of 0.02 eV/Å. We found this criterion to be a good compromise between calculation accuracy and computational cost. The force criterion is important because of the very flat potential energy surface of the water molecules. Reducing the force criterion to 0.01 eV/Å for a few test cases did not change the energy by more than 0.01 eV or the dipole moment by more than 5%.

The OH protonation calculations required a 4 × 3 Pt(111) unit cell in order to obtain an OH state in the presence of $H_5O_2^+$. The other parameters remained the same for these calculations.

To approximate the minimum energy path (MEP) for the reaction steps studied, several methods were used. When possible, the nudged elastic band (NEB) method[65] was used. For oxygen dissociation without the solution, the transition state image from the NEB calculation was optimized using the quasi-Newton method, which minimizes the forces to find the saddle point. The NEB method successfully found a transition state for O_2 protonation, but failed to converge for the other electrochemical steps (OOH dissociation, O protonation, OH diffusion, OH protonation). The extremely flat nature of the potential energy surface, in addition to the low energy barriers, severely complicates convergence of NEB calculations. For these calculations, a linear transit (LT) approach was used to approximate the MEP. In the LT calculations, intermediate points were interpolated between the two end points of a reaction. A geometry optimization was performed for each intermediate point in which one coordinate of the nonwater oxygen atom(s) was fixed, while all other nonmetal atoms were allowed to relax. In the region near the energy maximum, the intermediate points were spaced approximately 0.1 Å apart. The transition state obtained by the LT method is only an approximation of the saddle point, but considering the simple nature of the reaction pathways, the geometries and energies of the calculated transition states should be sufficiently close to those of the true transition state.

Energies are calculated with respect to a common reference state. Adsorption energies are calculated with reference to gas phase oxygen and a reference slab. For calculations without solution molecules, bare Pt(111) was taken as the reference, such that

$$\Delta E = E_{\mathrm{Pt-oxygen}} - E_{\mathrm{Pt}} - E_{\mathrm{O_2}}$$

Calculations with the solution molecules used the solution interacting with only Pt(111) as the reference. The adsorption energy, therefore, is calculated as

$$\Delta E = E_{\mathrm{adsorbate}} - E_{\mathrm{Pt-H_5O_2^+}} - xE_{\mathrm{O_2}}$$

where x is 1 for calculations originating from molecular oxygen and 1/2 for calculations originating from atomic oxygen. The term $E_{\mathrm{adsorbate}}$ refers to the energy of the states resulting from $H_5O_2^+$ coadsorbed with O or O_2. Transition state energies and reaction energies are calculated with reference to the initial state of the reaction.

It is important to note that the work function change with each reaction step indicates that the reactions do not take place at constant potential. Therefore, the potential of zero charge label is not applicable, even though no charge is added in these calculations. Calculations that consider effects of potential are currently being performed and will be presented in a subsequent publication.

Figure 1. $H_5O_2^+$ adsorbed on Pt(111).

3. Results

A. Nonelectrochemical Oxygen Dissociation. The nonelectrochemical dissociation of oxygen has been studied using DFT previously,[13−15,54,66,67] but is included here to provide a basis of comparison for the electrochemical calculations. Although two molecular oxygen precursor states and multiple atomic oxygen states are known to exist, only the dissociation precursor and the immediate dissociation product are presented. The dissociation precursor, O_2 bound in the top−fcc−bridge (tfb) site, adsorbs with an energy of −0.69 eV and an O−O distance of 1.39 Å at 1/9 ML coverage. This can be compared to −0.68 eV (bond distance 1.43 Å) found by Eichler et al. for the oxygen state in a $c(4\times2)$ coverage pattern.[13] The dissociation product, 2/9 ML of O adsorbed in the hcp sites, adsorbs with an energy of −1.28 eV. In comparing this to the work by Eichler et al. for a higher surface coverage (−0.98 eV), the lateral repulsions of oxygen atoms must be considered. We calculated the transition state to be 0.20 eV above the tfb adsorbed state with bond distance 2.15 Å. The energy compares favorably to the activation barrier estimated using time-resolved EEL spectra (0.29 eV),[17] though not to that calculated by Eichler et al. In the latter, the authors noted the discrepancy between their calculated barrier (0.86 eV)[13] and experiment. Finally, we calculated a work function change of −0.01 eV for the dissociation process, indicating a lack of charge transfer from the adsorbate to the metal during dissociation.

B. Electrochemical Oxygen Reduction Pathway. *I. The Solution Molecule.* As explained previously, we chose to model the solution as a Zundel cluster consisting of a proton solvated by two water molecules. In an acid solution, hydrogen bonding between the core water molecules and surrounding water molecules is certain to exist, resulting in a cluster with additional solvation. Nevertheless, the $H_5O_2^+$ structure provides a model for proton transfer at metal|solution interfaces in the mold of the UHV experiments performed by Wagner and Moylan.[40]

The adsorbed $H_5O_2^+$ cluster is bound to the Pt(111) surface through a hydrogen atom of one H_2O molecule directly above a surface Pt atom (see Figure 1). The other H_2O molecule resides between a bridge and a hollow site such that the oxygen−oxygen distance is 2.45 Å. This agrees well with the calculated solution phase simulation values of 2.4[49] and 2.39 Å.[68] Since the cluster is only weakly adsorbed on the surface, there is no preference toward orientation over the fcc hollow vs the hcp hollow. As in the solution phase, adsorbed $H_5O_2^+$ is nearly symmetric, with $O-H^+$ distances for the bound H_2O and "free" H_2O of 1.20 and 1.25 Å, respectively.

In the hydrogen electrode, adsorbed hydrogen desorbs from the electrode to the solution, forming a proton in the solution while donating an electron to the electrode. Wagner and Moylan,

TABLE 1: Calculated $H_5O_2^+$ Vibrational Mode Assignments on Pt(111)

mode	frequency (cm^{-1})
H^+ oscillation	1711, 1010
OH stretch	3647, 3260, 3202, 2493
H_2O scissoring	1591, 1521, 1377
libration	799, 753, 670, 552, 473, 200, 154, 76
H_2O rocking	306, 136, 102, 52

in their coadsorption experiments, asserted that $H_{ad} + H_2O_{ad}$ reacts to form H_3O^+ based on spectroscopic data[40] and the fact that neutral H_3O and H_5O_2 have been found to be unstable in the gas phase.[69] Our calculations reveal a decrease in the work function of 0.55 eV for the process of the adsorbed H (1/9 ML of H + H_2O dimer) reacting to form the Zundel cluster ($H_5O_2^+$). This work function change is significantly larger than the −0.04 eV change induced by 1/9 ML H adsorption, indicating significant transfer of negative charge to the metal. Despite the large work function change for the reaction, the ΔE is only 0.07 eV. Lackey et al. observed a ca. 0.1 eV work function decrease for the reaction on Pt(111) using 0.8 ML of H_2O and 0.6 ML of H in UHV.[70] The authors noted that the smaller than expected work function decrease is due to screening of the positive adsorbate charge by the excess water present. In this work, however, no excess water is included, so the work function calculated is the unscreened value.

Comparison of the experimental high-resolution EELS data with calculated vibrational data of the $H_5O_2^+$ cluster on Pt(111) gives further evidence that the experimentally observed structure is a Zundel or solvated Zundel cluster. As stated earlier, two vibrational modes indicate the presence of a proton on the surface: a mode at 1730 cm^{-1} on Pt(111),[40] 1680 cm^{-1} on Pt(110),[41] and 1690 cm^{-1} on Pt(100),[42] as well as an additional mode at 1150 cm^{-1} on all three surfaces. The oscillation of the proton perpendicular to the line between the two water molecules has been calculated to be 1711 cm^{-1}, while the oscillation of the proton along the same line is 1010 cm^{-1} (see Table 1). The OH stretches of the water molecules observed at 3440 cm^{-1} on Pt(111),[40] 3670 and 3410 cm^{-1} on Pt(110),[41] and 3430 cm^{-1} on Pt(100)[42] have been calculated as three modes at 3647, 3260, and 3202 cm^{-1}. The scissoring modes identified at 1620 cm^{-1} on Pt(111)[40] and Pt(110)[41] and 1645 cm^{-1} on Pt(100)[42] have been calculated to be two modes at 1591 and 1521 cm^{-1}. Our calculations indicate that further solvation of the Zundel cluster increases the low frequency proton oscillation by nearly 70 cm^{-1}. Additionally, based on our calculations, an Eigen-like cluster would have vibrational modes in the range of 2400−2800 cm^{-1}. Neither the UHV nor IRAS studies detected a mode in this range.

II. Elementary Oxygen Reduction Reaction Steps. Numerous surface structures involving the Zundel molecule and possible intermediates in the oxygen reduction reaction were investigated in this study. Below, we report results for only the most stable intermediates, focusing on the elementary reaction steps of the most favorable ORR pathway. These steps are O_2 protonation, OOH dissociation, O protonation, OH diffusion, and OH protonation. Other possible steps and pathways are addressed in the Discussion section.

The proton transfer steps are expected to be very rapid based on solution phase proton transfer. The activation energy of a Zundel to Zundel proton transfer was found to be 0.07 eV,[49] with an apparent activation energy of proton diffusion through water of 0.11 eV.[50] No calculations concerning the intermediate solvent reorganization steps that occur prior to each protonation step have been performed in the present work. This is important because a fast proton transfer step may be followed by a comparatively slow solvent reorganization step, as in proton transfer in acid solutions.[50] However, even at 130 K, H_2O diffusion on Pt(111) is rapid.[71,72]

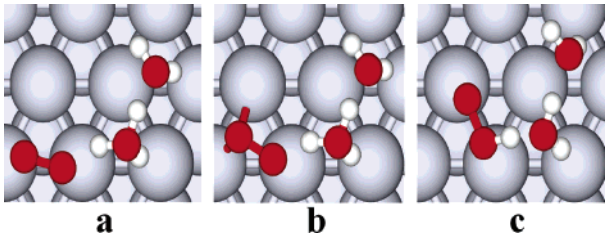

Figure 2. O_2 protonation on Pt(111): (a) $O_2/H_5O_2^+$ adsorption; (b) transition state; (c) $OOH/(H_2O)_2$ adsorption.

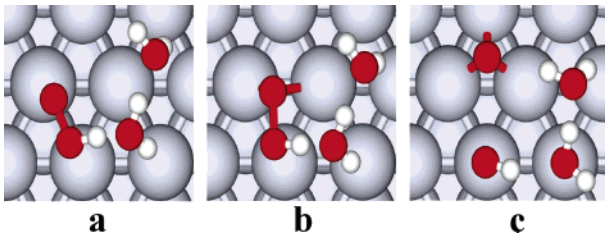

Figure 3. OOH dissociation on Pt(111): (a) OOH adsorption; (b) transition state; (c) dissociated state, i.e., $(OH + O)/(H_2O)_2$ adsorption.

(i) Protonation of O_2. In the presence of $H_5O_2^+$, O_2 adsorbs in a bridge site between two Pt atoms with an adsorption energy of −0.96 eV. Spin polarization was found to have a negligible effect on the energy. The 1.72 Å distance between O_2 and the H atom of $H_5O_2^+$ indicates a hydrogen bond between the adsorbate and the solution, which induces a slight reorientation of $H_5O_2^+$. In this reorientation process, the distance between the proton and the water molecule adjacent to O_2 decreases to 1.10 Å, while the distance between the proton and the second water molecule increases to 1.39 Å. Proton transfer to O_2 is accompanied by a rotation of the oxygen−oxygen bond across the hollow site toward the $H_5O_2^+$ cluster (see Figure 2). The OOH (peroxy) state resulting from proton transfer resides on the bridge site with an adsorption energy of −1.19 eV, which is not affected by spin polarization. In the proton transfer process, the distance from the oxygen molecule to the water molecule decreases from 2.66 to 2.47 Å as measured by the distance between the two closest oxygen atoms. This process has an early transition state with energy 0.07 eV above the reactant state and an O−H bond length of 1.63 Å. The O−H bond distance in the peroxy state is 1.13 Å, while the H−H_2O bond distance is 1.34 Å, an increase from 1.02 Å in the O_2 state. Accompanying the proton transfer process is a work function change from 5.03 eV for adsorbed O_2 to 5.52 eV for OOH, indicating electron transfer from the metal surface to the adsorbate. This work function change is very close in magnitude to the −0.55 eV work function change for the proton formation reaction.

(ii) Dissociation of OOH. As in the oxygen protonation step, an early transition state is observed (see Figure 3), which is 0.22 eV above the OOH state. The unprotonated oxygen atom in OOH moves toward the dissociated state, lengthening the O−O bond from 1.48 to 1.65 Å in the transition state, while the H−H_2O bond enlarges to 1.53 Å. The solution itself does not reorient at this state. After the transition state, the solution reorients rather significantly, as the water molecule closest to the OH adsorbate becomes oriented oxygen down, rather than hydrogen down, with the oxygen atom of the aforementioned water molecule moving from 3.18 Å above the Pt surface to

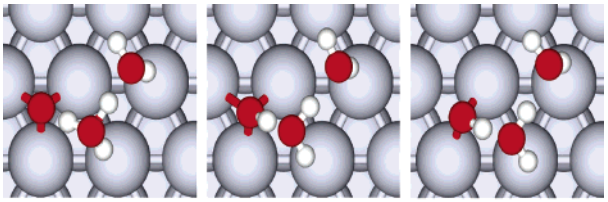

Figure 4. O protonation on Pt(111): (a) $O/H_5O_2^+$ adsorption; (b) transition state; (c) $OH/(H_2O)_2$ adsorption.

2.31 Å above the surface. However, the distance between oxygen atoms in the two water molecules does not change. The adsorption energy for the dissociated state is −2.24 eV, which is significantly larger in magnitude than the OOH state, while the work function of the dissociated state is 5.30 eV, 0.22 eV less than OOH. Since O_2 dissociation results in a negligible work function change, the work function decrease in OOH dissociation may be a result of solution reorientation rather than electron donation to the oxygen species. That is, the work function change is due to the formation of a H_2O-Pt bond. Solution reorientation may also explain the larger ΔE of OOH dissociation (−1.05 eV) compared to O_2 dissociation (−0.59 eV).

(iii) Protonation of Atomic Oxygen. The products of peroxy dissociation (O + OH) must be protonated further to form H_2O. Following OOH dissociation, the adsorbed O atom is not solvated; a diffusion step must take place before it can be protonated. The O diffusion barrier on Pt(111) has been calculated to be 0.58 eV,[73] and is static compared to H_2O diffusion,[72] indicating that $H_5O_2^+$ diffuses and not O.

The adsorption energy of solvated O is −1.29 eV, which is 0.14 eV more stable than unsolvated O at the same coverage. Structurally, the solution behaves similarly in O protonation to O_2 protonation (see Figure 4). To reach the transition state, the adsorbed oxygen moves 0.15 Å toward the solution cluster, while the nearest H from $H_5O_2^+$ moves 0.08 Å toward the adsorbed oxygen. This small movement results in a small transition state energy of 0.03 eV above the adsorbed oxygen. The OH product adsorbs in the bridge site 0.62 Å from the initial oxygen position, with a final O−H bond length of 1.03 Å. The energy change of protonation of atomic oxygen, though, is −0.07 eV, which is significantly smaller than the −0.24 eV of molecular oxygen protonation. Protonation of O, like protonation of O_2, is accompanied by a significant work function change from 4.96 to 5.66 eV, indicating that charge is transferred from the metal to the adsorbate.

(iv) Protonation of Adsorbed OH. Surface OH is produced from both OOH dissociation and O protonation, albeit in different states. Atop adsorbed OH, produced from OOH dissociation, is −0.10 eV more stable than bridge bonded OH, which is produced by O protonation. Additionally, atop adsorbed OH has a work function of 5.22 eV compared to 5.67 eV for bridge bonded OH. More importantly, bridge bonded OH is unable to accept a proton according to our calculations. When $H_5O_2^+$ diffuses toward bridge bonded OH, OH diffuses to the atop site before proton transfer occurs. As such, following O protonation, OH must diffuse to the atop state, overcoming a barrier of 0.13 eV. Although OH in these calculations is solvated by a water dimer, the activation barrier is very close to the barrier for nonsolvated OH diffusion of 0.11 eV calculated by Michaelides and Hu.[25] A discrepancy in the diffusion energy change is observed (Michaelides and Hu calculated the change to be −0.02 eV), but this can be explained by the formation of a weak bond between the dimer and the Pt surface in the atop state.

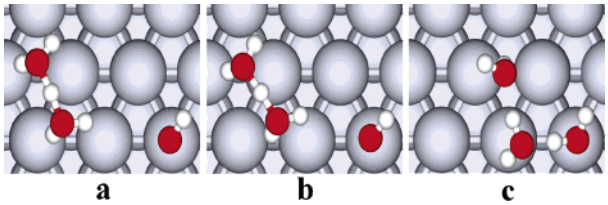

Figure 5. OH protonation on Pt(111): (a) $OH/H_5O_2^+$; (b) transition state; (c) $(H_2O)_3$.

Both OOH dissociation and O protonation result in solvated OH. Because of the strong interaction between OH and H_2O, breaking the OH−dimer bond may require considerable energy. Our calculations indicate that, on Pt(111), breaking the $OH-(H_2O)_2$ bond costs 0.10 eV. Previously, however, the hydrogen bond between adsorbed H_2O and OH on Pt(111) was calculated to be −0.44 eV.[74] Without hydrogen bonding to the adsorbed OH, the dimer may interact more strongly with the Pt surface. Regardless, the activation barrier for breaking the hydrogen bond is significant, and OH likely remains solvated during proton transfer (i.e., $OH-(H_2O)_2 + H_5O_2^+ + e^- \rightarrow (H_2O)_5$). However, to simplify the model and to maintain consistency with the previous calculations, the adsorbed OH does not include the solvating dimer prior to protonation (i.e., $OH + H_5O_2^+ + e^- \rightarrow (H_2O)_3$).

Following OOH dissociation or OH diffusion to the atop site, OH does not interact with $H_5O_2^+$. $H_5O_2^+$ must first migrate on the surface toward OH before the reaction can take place. In their adsorbed states prior to reacting, $H_5O_2^+$ and OH are separated by 3.71 Å. As $H_5O_2^+$ moves toward the adsorbed OH, the energy increases by only 0.01 eV above the initial state (see Figure 5). At the energy maximum, the cluster−OH distance is reduced to 3.19 Å. Once the cluster−OH distance becomes smaller than that at the transition state, the attraction between the cluster and the OH induces proton transfer. These results suggest that proton transfer to hydroxyl groups is essentially instantaneous unless solvent reorganization is slow. The result of the reaction is three strongly hydrogen bonded water molecules. The energy change for the water trimer formation reaction is −0.92 eV, which is significantly more exothermic than the previous proton transfer steps. As in the other proton transfer steps, the work function increase from 4.97 to 5.25 eV indicates electron transfer to the surface. However, the reorientation of the water molecules precludes making a quantitative comparison of the work function changes. To complete the oxygen reduction, one of the molecules in the trimer must desorb from the surface, forming a dimer. This dimer can then accept a proton from the solution and form a new $H_5O_2^+$ cluster. The energy change for H_2O desorption into vacuum is 0.54 eV. In an aqueous environment, H_2O desorbs into the solution phase, where there is significant hydrogen bonding between molecules. Taking the difference in energy between H_2O liquid and vapor to be −0.46 eV, the value at 298 K, the ΔE of H_2O desorption in solution is 0.08 eV.

4. Discussion

In the preceding section, the results of calculations were reported for five elementary steps—proton transfer to O_2, OOH dissociation, proton transfer to O, OH diffusion, and proton transfer to OH—which were found to represent the most favorable water formation pathway in our calculations (see Table 2). Below, we compare the reaction pathway identified above

TABLE 2: Activation Barriers (ΔE^{TS}) and Reaction Enthalpies (ΔE) for the ORR

	ΔE^{TS} (eV)	ΔE (eV)
O_2 protonation	0.07	−0.23
OOH dissociation	0.22	−1.05
O protonation	0.03	−0.07
OH (bridge) diffusion	0.13	−0.10
OH (atop) protonation	0.01	−0.92

with alternate proposed pathways. We also address possible origins of the large overpotential observed for the oxygen reduction reaction.

A. O_2 Protonation vs O_2 Dissociation as the Initial ORR Step. The calculations reported here, in conjunction with information previously known, suggest that the presence of the solution alters the pathway of oxygen reduction on Pt(111). When O_2 adsorbs on Pt(111) in the presence of $H_5O_2^+$, a hydrogen bond forms between the molecules, such that O_2 is 0.27 eV more stable than the unsolvated O_2 dissociation precursor. This strong interaction between O_2 and $H_5O_2^+$ appears to prevent the dissociation of O_2, since our calculations yielded no reasonable O_2 dissociation pathway in the presence of $H_5O_2^+$. Kinetically, O_2 protonation is more favorable than dissociation based on its lower activation barrier. Although direct O_2 dissociation in the ORR cannot be precluded, the results reported do suggest that the electrochemical ORR proceeds through the pathway proposed by Damjanovic in which the proton transfer precedes dissociation.[7]

B. Formation of Peroxide. It is known that oxygen can be reduced to H_2O_2 on Pt electrodes. In this scenario, OOH accepts a proton rather than dissociating. One interpretation of this is that the ORR proceeds through an adsorbed H_2O_2 intermediate. However, several observations offer another explanation. Markovic et al. performed rotating ring disk electrode (RRDE) experiments in 0.1 M $HClO_4$ with and without 1×10^{-4} M KBr.[75] H_2O_2 was detected only in the experiments with KBr, apparently due to adsorbed Br blocking sites necessary for breaking the O−O bond without inhibiting O_2 adsorption. Additionally, our calculations with solvating water molecules, but without any site blocking adsorbates, showed that H_2O_2 is unstable on Pt(111) and dissociates into two OH adsorbates. DFT calculations by Panchenko et al. on the (111), (110), and (100) faces of Pt without solvation found adsorbed H_2O_2 to be unstable as well.[66] The RRDE experiments and DFT calculations suggest that OOH can be protonated only when dissociation is inhibited by neighboring adsorbates.

C. Accumulation of Surface Oxygenates at High Potentials. As mentioned previously, it has been proposed that adsorbed OH molecules block surface sites for oxygen reduction as well as affect the reaction energetics.[9] Experiments using 1 and 6 M CF_3SO_3H electrolytes suggest that the OH molecules adsorbed at high electrode potentials are a result of H_2O decomposition.[10] Based on the results of the calculations presented in the previous section, a barrier of 0.93 eV must be overcome for $(H_2O)_3$ to form an adsorbed OH plus $H_5O_2^+$. This large energy barrier would seem to prohibit H_2O decomposition. Rather than breaking an O−H bond, more likely, the water trimer would decompose into a dimer and a monomer, since the hydrogen bonding between two water molecules has an energy of only −0.21 eV.[74] Additionally, Michaelides and Hu calculated the activation barrier of $H_2O_{ad} \rightarrow OH_{ad} + H_{ad}$ on Pt(111) to be 0.68 eV,[26] significantly less than H^+ formation from $(H_2O)_3$. At potentials > 0 V vs RHE, H_{ad} rapidly forms H^+. This information suggests the existence of an alternate pathway that is more favorable than $(H_2O)_3 \rightarrow H_5O_2^+ + e^- + OH$.

An alternate explanation of the accumulation of adsorbed OH molecules is that the reaction stalls in the adsorbed O and OH (bridge) states following OOH dissociation. Considering no potential effects, the barrier for OH deprotonation is less (0.08 eV) than the barrier for OH diffusion to the atop site (0.13 eV). At high potentials, this effect could be even more drastic. The dipole moment change for the deprotonation reaction is −1.27 D, compared to −0.72 D for OH diffusion, meaning the interaction of positive electric fields at the cathode would stabilize the adsorption of O compared with OH.[54] As potential increases, the equilibrium changes to favor accumulation of O on the surface. Our work examining the effects of electrode potential on the reaction steps examined here is currently in progress and will be published in the future.

Supporting evidence is found in the work by Zhang et al.[76] In this work, the authors found that the suitability of a catalyst for ORR can be evaluated by its propensity to both break the oxygen−oxygen bond and hydrogenate atomic oxygen. Stated another way, in selecting an ORR catalyst, the ability of the catalyst to dissociate oxygen must be weighed against its tendency to accumulate atomic oxygen on the surface. While Zhang and coauthors did not consider the role of solvation, their findings are consistent with the present work, in that OOH dissociation and OH (de)protonation are the steps that kinetically limit the electrocatalytic oxygen reduction.

5. Conclusions

Although the structure of the electrode|solution interface in acid electrolytes is not precisely known, numerous electrochemical and ultrahigh vacuum studies, as well as aqueous phase simulations of acids, have advanced the knowledge of the interface. We constructed the UHV model of the electrode|solution interface to study the oxygen reduction reaction on Pt(111) using DFT. With DFT, we have extended the ultrahigh vacuum approach to study electrochemical reactions on the surface that would otherwise be forbidden due to temperature constraints.

Using an $H_5O_2^+$ cluster to simulate the acid solution, we determined that O_2 protonation has a more stable precursor and lower activation barrier than O_2 dissociation. This information, combined with facile proton transfer and water diffusion, implicates the Damjanovic pathway in which proton transfer precedes O−O dissociation and is accompanied by electron transfer. After the initial proton transfer step, OOH dissociates with a barrier similar to O_2 dissociation, although OOH dissociation is significantly more exothermic. We speculate that the additional energy liberated during this reaction results from the reorientation of the solution molecules. The atop adsorbed OH readily accepts a proton to form water, leaving adsorbed O on the surface. After a diffusion step in which O becomes solvated by $H_5O_2^+$ cluster, an approximately barrierless proton transfer step occurs to produce OH. This bridge bonded OH state must diffuse to the atop site before it can accept a proton. After diffusion, proton transfer again occurs, completing the reaction.

All of the steps studied have very low activation barriers, the highest being 0.22 eV. Additionally, all of the steps are exothermic, so no step is thermodynamically unfavorable. It should be expected from these data that the ORR is a very fast reaction, which is known not to be the case. More careful examination reveals that the inability of bridge bonded OH to accept protons may throttle the O protonation pathway, which

would cause O or OH to accumulate on the surface. This throttling is likely exacerbated at high potentials, since O(H) coverage of the electrode surface increases with electrode potential. More work is necessary to understand the effects of electrode potential, as well as the effect of coadsorbed oxygen species, on the reaction steps studied in this work.

Acknowledgment. M.P.H. acknowledges support from a U.S. Department of Education GAANN Fellowship. This research was supported in part by the National Science Foundation through the San Diego Supercomputer Center under grant CHE040030 using DataStar.

References and Notes

(1) Mukerjee, S.; Srinivasan, S.; Soriaga, M. P.; Mcbreen, J. *J. Phys. Chem.* **1995**, *99*, 4577.
(2) Mukerjee, S.; Srinivasan, S.; Soriaga, M. P.; McBreen, J. *J. Electrochem. Soc.* **1995**, *142*, 1409.
(3) Paulus, U. A.; Wokaun, A.; Scherer, G. G.; Schmidt, T. J.; Stamenkovic, V.; Radmilovic, V.; Markovic, N. M.; Ross, P. N. *J. Phys. Chem. B* **2002**, *106*, 4181.
(4) Stamenkovic, V.; Schmidt, T. J.; Ross, P. N.; Markovic, N. M. *J. Phys. Chem. B* **2002**, *106*, 11970.
(5) Yeager, E.; Razaq, M.; Gervasio, D.; Razak, A.; Tryk, A. D. The electrolyte factor in O_2 reduction electrocatalysis. *Proceedings of the Workshop on Structural Effects in Electrocatalysis and Oxygen Electrochemistry*, The Electrochemical Society: Pennington, NJ, 1992; pp 440−473.
(6) Adzic, R. R. Recent Advances in the Kinetics of Oxygen Reduction. In *Electrocatalysis*; Lipkowski, J., Ross, P. N., Eds.; Wiley-VCH: New York, 1998; p 197.
(7) Damjanovic, A.; Brusic, V. *Electrochim. Acta* **1967**, *12*, 615.
(8) Damjanovic, A. Progress in the Studies of Oxygen Reduction during the Last Thirty Years. In *Electrochemistry in Transition*; Murphy, O. J., Srinivasan, S., Conway, B. E., Eds.; Plenum Press: New York, 1992; p 107.
(9) Sepa, D. B.; Vojnovic, M. V.; Damjanovic, A. *Electrochim. Acta* **1981**, *26*, 781.
(10) Murthi, V. S.; Urian, R. C.; Mukerjee, S. *J. Phys. Chem. B* **2004**, *108*, 11011.
(11) Markovic, N. M.; Gasteiger, H. A.; Ross, P. N. *J. Phys. Chem.* **1995**, *99*, 3411.
(12) Ghoneim, M. M.; Clouser, S.; Yeager, E. *J. Electrochem. Soc.* **1985**, *132*, 1160.
(13) Eichler, A.; Hafner, J. *Phys. Rev. Lett.* **1997**, *79*, 4481.
(14) Eichler, A.; Mittendorfer, F.; Hafner, J. *Phys. Rev. B* **2000**, *62*, 4744.
(15) Sljivancanin, Z.; Hammer, B. *Surf. Sci.* **2002**, *515*, 235.
(16) Nolan, P. D.; Lutz, B. R.; Tanaka, P. L.; Davis, J. E.; Mullins, C. B. *Phys. Rev. Lett.* **1998**, *81*, 3179.
(17) Nolan, P. D.; Lutz, B. R.; Tanaka, P. L.; Davis, J. E.; Mullins, C. B. *J. Chem. Phys.* **1999**, *111*, 3696.
(18) Gland, J. L. *Surf. Sci.* **1980**, *93*, 487.
(19) Gland, J. L.; Sexton, B. A.; Fisher, G. B. *Surf. Sci.* **1980**, *95*, 587.
(20) Gland, J. L.; Korchak, V. N. *Surf. Sci.* **1978**, *75*, 733.
(21) Luntz, A. C.; Grimblot, J.; Fowler, D. E. *Phys. Rev. B* **1989**, *39*, 12903.
(22) Gland, J. L.; Fisher, G. B.; Kollin, E. B. *J. Catal.* **1982**, *77*, 263.
(23) Creighton, J. R.; White, J. M. *Chem. Phys. Lett.* **1982**, *92*, 435.
(24) Fisher, G. B.; Gland, J. L.; Schmieg, S. J. *J. Vac. Sci. Technol.* **1982**, *20*, 518.
(25) Michaelides, A.; Hu, P. *J. Chem. Phys.* **2001**, *114*, 513.
(26) Michaelides, A.; Hu, P. *J. Am. Chem. Soc.* **2001**, *123*, 4235.
(27) Mitchell, G. E.; Akhter, S.; White, J. M. *Surf. Sci.* **1986**, *166*, 283.
(28) Mitchell, G. E.; Akhter, S.; White, J. M. *J. Vac. Sci. Technol., A* **1986**, *4*, 1472.
(29) Ogle, K. M.; White, J. M. *Surf. Sci.* **1986**, *169*, 425.
(30) Ogle, K. M.; White, J. M. *Surf. Sci.* **1984**, *139*, 43.
(31) Ogle, K. M.; Creighton, J. R.; Luftman, H. S.; White, J. M. *J. Chem. Phys.* **1983**, *78*, 5839.
(32) Trasatti, S. The Electrode Potential. In *Comprehensive Treatise of Electrochemistry*; Bockris, J. O. M., Conway, B. E., Yeager, E., Eds.; Plenum Press: New York and London, 1980; Vol. 1, p 45.
(33) Bockris, J. O. M.; Reddy, A. K. N.; Gamboa-Aldeco, M. *Modern Electrochemistry: Fundamentals of Electrodics*, 2nd ed.; Plenum Publishers: New York, 2000; Vol. 2A.
(34) Wagner, F. T. Simulation of the Electrical Double-Layer in Ultrahigh Vacuum. In *Structure of Electrified Interfaces*; Lipkowski, J., Ross, P. N., Eds.; VCH: New York, 1993.
(35) Vassilev, P.; van Santen, R. A.; Koper, M. T. M. *J. Chem. Phys.* **2005**, *122*, 054701.
(36) Ogasawara, H.; Brena, B.; Nordlund, D.; Nyberg, M.; Pelmenschikov, A.; Pettersson, L. G. M.; Nilsson, A. *Phys. Rev. Lett.* **2002**, *89*, 276102.
(37) Jorgensen, W. L. *J. Chem. Phys.* **1982**, *77*, 4156.
(38) Brubach, J. B.; Mermet, A.; Filabozzi, A.; Gerschel, A.; Roy, P. *J. Chem. Phys.* **2005**, *122*, 184509.
(39) Lofgren, P.; Kasemo, B. *Catal. Lett.* **1998**, *53*, 33.
(40) Wagner, F. T.; Moylan, T. E. *Surf. Sci.* **1988**, *206*, 187.
(41) Chen, N.; Blowers, P.; Masel, R. I. *Surf. Sci.* **1999**, *419*, 150.
(42) Kizhakevariam, N.; Stuve, E. M. *Surf. Sci.* **1992**, *275*, 223.
(43) Hirota, K.; Song, M. B.; Ito, M. *Chem. Phys. Lett.* **1996**, *250*, 335.
(44) Olivera, P. P.; Ferral, A.; Patrito, E. M. *J. Phys. Chem. B* **2001**, *105*, 7227.
(45) de Grotthuss, C. J. T. *Ann. Chim.* **1806**, *58*, 54.
(46) Zundel, G. In *The Hydrogen Bond—Recent Developments in Theory and Experiments. II. Structure and Spectroscopy*; Schuster, P., Zundel, G., Sandorfy, C., Eds.; North-Holland Publishing Company: Amsterdam, 1976, pp 683−766.
(47) Eigen, M. *Angew. Chem., Int. Ed.* **1964**, *3*, 1.
(48) Marx, D.; Tuckerman, M. E.; Hutter, J.; Parrinello, M. *Nature* **1999**, *397*, 601.
(49) Kornyshev, A. A.; Kuznetsov, A. M.; Spohr, E.; Ulstrup, J. *J. Phys. Chem. B* **2003**, *107*, 3351.
(50) Agmon, N. *Chem. Phys. Lett.* **1995**, *244*, 456.
(51) Headrick, J. M.; Diken, E. G.; Walters, R. S.; Hammer, N. I.; Christie, R. A.; Cui, J.; Myshakin, E. M.; Duncan, M. A.; Johnson, M. A.; Jordan, K. D. *Science* **2005**, *308*, 1765.
(52) Hohenberg, P.; Kohn, W. *Phys. Rev.* **1964**, *136*, B864.
(53) Payne, M. C.; Teter, M. P.; Allan, D. C.; Arias, T. A.; Joannopoulos, J. D. *Rev. Mod. Phys.* **1992**, *64*, 1045.
(54) Hyman, M. P.; Medlin, J. W. *J. Phys. Chem. B* **2005**, *109*, 6304.
(55) Lee, G.; Plummer, E. W. *Phys. Rev. B* **1995**, *51*, 7250.
(56) Sheth, P. A.; Neurock, M.; Smith, C. M. *J. Phys. Chem. B* **2005**, *109*, 12449.
(57) Rothfuss, C. J.; Medvedev, V. K.; Stuve, E. M. *Surf. Sci.* **2002**, *501*, 169.
(58) Kresse, G.; Hafner, J. *Phys. Rev. B* **1993**, *47*, 558.
(59) Kresse, G.; Furthmuller, J. *Comput. Mater. Sci.* **1996**, *6*, 15.
(60) Kresse, G.; Furthmuller, J. *Phys. Rev. B* **1996**, *54*, 11169.
(61) Blochl, P. E. *Phys. Rev. B* **1994**, *50*, 17953.
(62) Kresse, G.; Joubert, D. *Phys. Rev. B* **1999**, *59*, 1758.
(63) Perdew, J. P.; Chevary, J. A.; Vosko, S. H.; Jackson, K. A.; Pederson, M. R.; Singh, D. J.; Fiolhais, C. *Phys. Rev. B* **1992**, *46*, 6671.
(64) Monkhorst, H. J.; Pack, J. D. *Phys. Rev. B* **1976**, *13*, 5188.
(65) Jónsson, H.; Mills, G.; Jacobsen, K. W. Nudged Elastic Band Method for Finding Minimum Energy Paths of Transitions. In *Classical and Quantum Dynamics in Condensed Phase Simulations*; Berne, B. J., Ciccotti, G., Coker, D. F., Eds.; World Scientific: Singapore, 1998; p 385.
(66) Panchenko, A.; Koper, M. T. M.; Shubina, T. E.; Mitchell, S. J.; Roduner, E. *J. Electrochem. Soc.* **2004**, *151*, A2016.
(67) Watwe, R. M.; Cortright, R. D.; Mavrikakis, M.; Norskov, J. K.; Dumesic, J. A. *J. Chem. Phys.* **2001**, *114*, 4663.
(68) Corongiu, G.; Kelterbaum, R.; Kochanski, E. *J. Phys. Chem.* **1995**, *99*, 8038.
(69) Gellene, G. I.; Porter, R. F. *J. Chem. Phys.* **1984**, *81*, 5570.
(70) Lackey, D.; Schott, J.; Sass, J. K.; Woo, S. I.; Wagner, F. T. *Chem. Phys. Lett.* **1991**, *184*, 277.
(71) Sachs, C.; Hildebrand, M.; Volkening, S.; Wintterlin, J.; Ertl, G. *J. Chem. Phys.* **2002**, *116*, 5759.
(72) Nagasaka, M.; Kondoh, H.; Ohta, T. *J. Chem. Phys.* **2005**, *122*, 204704.
(73) Bogicevic, A.; Stromquist, J.; Lundqvist, B. I. *Phys. Rev. B* **1998**, *57*, R4289.
(74) Karlberg, G. S.; Wahnstrom, G. *Phys. Rev. Lett.* **2004**, *92*, 046102.
(75) Markovic, N. M.; Gasteiger, H. A.; Grgur, B. N.; Ross, P. N. *J. Electroanal. Chem.* **1999**, *467*, 157.
(76) Zhang, J. L.; Vukmirovic, M. B.; Xu, Y.; Mavrikakis, M.; Adzic, R. R. *Angew. Chem., Int. Ed.* **2005**, *44*, 2132.